

AD-A074 896

AEROSPACE CORP EL SEGUNDO CA VEHICLE ENGINEERING DIV F/G 20/13
PHASE CHANGE HEAT CONDUCTION IN GENERAL ORTHOGONAL CURVILINEAR --ETC(U)
FEB 79 L BLEDJIAN F04701-78-C-0079
TR-0079(4901-01)-1

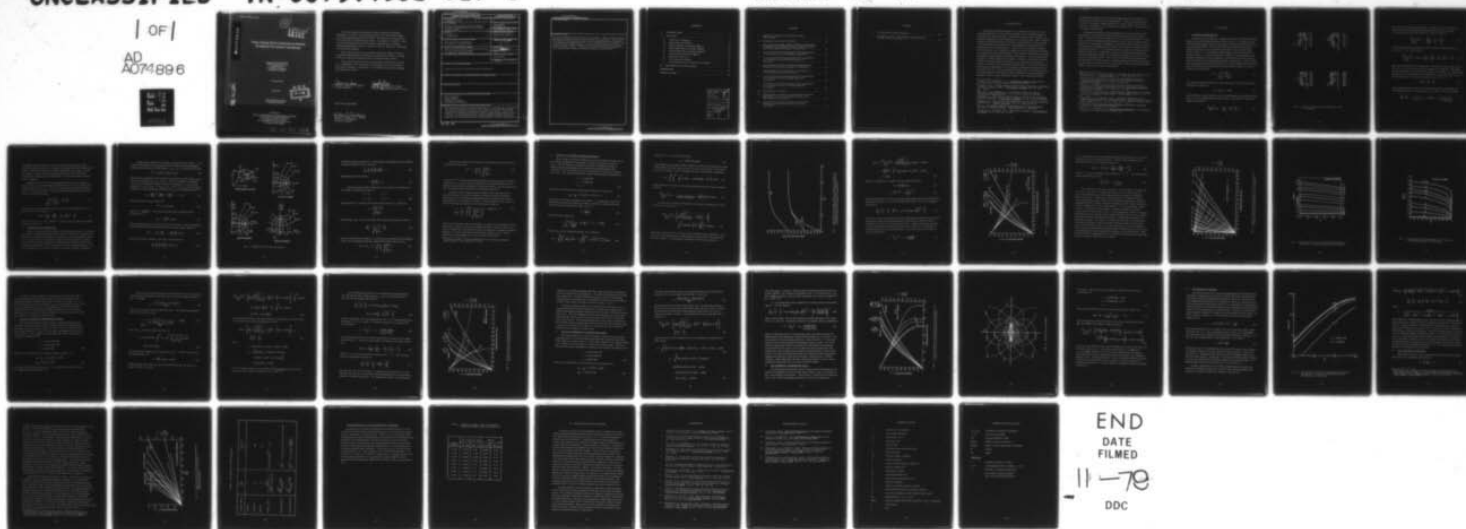
UNCLASSIFIED

SAMSO-TR-79-81

NL

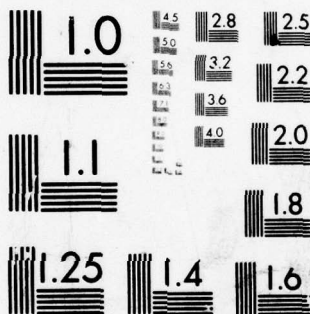
| OF |

AD
A074896



END
DATE
FILMED

11-79
DDC



MICROCOPY RESOLUTION TEST CHART
NATIONAL BUREAU OF STANDARDS-1963-A

AD A074896

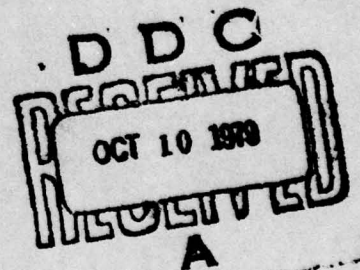
12
LEVEL

Phase Change Heat Conduction in General Orthogonal Curvilinear Coordinates

Prepared by LEON BLEDJIAN
Vehicle Engineering Division
Engineering Group
The Aerospace Corporation
El Segundo, Calif. 90245

15 February 1979

Final Report



DDC FILE COPY

APPROVED FOR PUBLIC RELEASE;
DISTRIBUTION UNLIMITED


Prepared for
SPACE AND MISSILE SYSTEMS ORGANIZATION
AIR FORCE SYSTEMS COMMAND
Los Angeles Air Force Station
P.O. Box 92960, Worldway Postal Center
Los Angeles, Calif. 90009

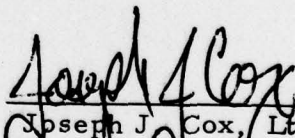
79 10 09 056

This final report was submitted by The Aerospace Corporation, El Segundo, CA 90245, under Contract F04701-78-C-0079 with the Space and Missile Systems Organization (AFSC), Los Angeles Air Force Station P.O. Box 92960, Worldway Postal Center, Los Angeles, CA 90009. It was reviewed and approved for The Aerospace Corporation by D. Willens, Vehicle Engineering Division. Lt. James C. Garcia, Deputy for Technology, was the project engineer.

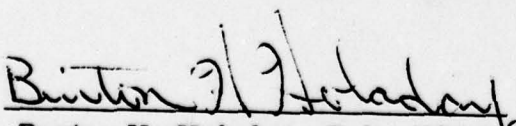
This report has been reviewed by the Information Office (OI) and is releasable to the National Technical Information Service (NTIS). At NTIS, it will be available to the general public, including foreign nations.

This technical report has been reviewed and is approved for publication. Publication of this report does not constitute Air Force approval of the report's findings or conclusions. It is published only for the exchange and stimulation of ideas.


James C. Garcia, Lt., USAF
Project Engineer


Joseph J. Cox, Lt. Col., USAF
Chief, Advanced Technology Division

FOR THE COMMANDER


Burton H. Holaday, Col., USAF
Director of Technology,
Plans and Analysis

UNCLASSIFIED

SECURITY CLASSIFICATION OF THIS PAGE (When Data Entered)

REPORT DOCUMENTATION PAGE		READ INSTRUCTIONS BEFORE COMPLETING FORM	
1. REPORT NUMBER SAMSO-TR-79-81	2. GOVT ACCESSION NO.	3. RECIPIENT'S CATALOG NUMBER	
4. TITLE (and Subtitle) PHASE CHANGE HEAT CONDUCTION IN GENERAL ORTHOGONAL CURVILINEAR COORDINATES.	5. TYPE OF REPORT & PERIOD COVERED Final Report. 1967-68 1968	6. PERFORMING ORG. REPORT NUMBER TR-0079(4901-01)-1	
7. AUTHOR(s) Leon Bledjian	8. CONTRACT OR GRANT NUMBER(s) F04701-78-C-0079	9. PERFORMING ORGANIZATION NAME AND ADDRESS The Aerospace Corporation El Segundo, California 90245	10. PROGRAM ELEMENT, PROJECT, TASK AREA & WORK UNIT NUMBERS 12 50
11. CONTROLLING OFFICE NAME AND ADDRESS Space and Missile Systems Organization/DVXT Air Force Systems Command Los Angeles, California 90045	12. REPORT DATE 15 Feb 1979	13. NUMBER OF PAGES 46	
14. MONITORING AGENCY NAME & ADDRESS (if different from Controlling Office)	15. SECURITY CLASS. (of this report) Unclassified	15a. DECLASSIFICATION/DOWNGRADING SCHEDULE	
16. DISTRIBUTION STATEMENT (of this Report) Approved for public release; distribution unlimited.			
17. DISTRIBUTION STATEMENT (of the abstract entered in Block 20, if different from Report)			
18. SUPPLEMENTARY NOTES			
19. KEY WORDS (Continue on reverse side if necessary and identify by block number) Heat Conduction Phase Change Melting or Freezing Generalized Coordinates			
20. ABSTRACT (Continue on reverse side if necessary and identify by block number) The approximate method of London and Seban for predicting the solidification rate and for melting in or around slabs, cylinders, and spheres has been reformulated in general orthogonal curvilinear coordinates. Closed-form solutions are presented for the rate of phase change and temperature drop as a function of a nondimensional time, $SteFo$ (product of Stefan and Fourier numbers), for various geometries including elliptic cylinders, spheroids of			

DD FORM 1473
(FACSIMILE)

UNCLASSIFIED 409 369

SECURITY CLASSIFICATION OF THIS PAGE (When Data Entered)

UNCLASSIFIED

SECURITY CLASSIFICATION OF THIS PAGE(When Data Entered)

19. KEY WORDS (Continued)

20. ABSTRACT (Continued)

varying eccentricities, and bicylindrical problems. Both convection and flux boundary conditions which can vary with time are considered. The effect of Biot number on phase change times and the resulting boundary temperature are presented in graphical form for some of the geometries considered. The method's degree of approximation is investigated by comparison with published analytical results. The approximate applicability of the equations to some special phase change conduction problems is demonstrated.

UNCLASSIFIED

SECURITY CLASSIFICATION OF THIS PAGE(When Data Entered)

CONTENTS

I.	INTRODUCTION	5
II.	ANALYSIS	7
A.	Cartesian Coordinates	7
B.	Generalized Coordinates	10
C.	Elliptic Cylinder Coordinates (η, θ, z)	15
D.	Oblate Spheroidal Coordinates (η, θ, ψ)	24
E.	Prolate Spheroidal Coordinates (η, θ, ψ)	29
F.	Bicylindrical Coordinates (η, ψ, z)	31
G.	Estimation of Errors	35
H.	Flux Boundary Condition	37
I.	Approximation of Two-Dimensional Problems	41
III.	DISCUSSION AND CONCLUSIONS	43
	REFERENCES	45
	NOMENCLATURE	47

Accession For	
NTIS GRA&I	<input checked="checked" type="checkbox"/>
DDC TAB	<input type="checkbox"/>
Unannounced	<input type="checkbox"/>
Justification _____	
By _____	
Distribution/ _____	
Availability Codes	
Dist	Avail and/or special
A	

FIGURES

1.	Idealized Temperature Distributions during Phase Change	8
2.	Orthogonal Curvilinear Coordinates	12
3.	Special Functions $E(\eta)$, $I_o(\eta)$ and $I_p^{-1}(\eta)$ to Facilitate the Computation of the Elliptic Cylinder, Oblate Spheroidal and Prolate Spheroidal Results, Respectively	17
4.	Frozen Fraction and Dimensionless Wall Temperature as a Function of Time for Elliptic Coordinates	19
5.	Frozen Fraction and Dimensionless Wall Temperature as a Function of Time with Biot Number as a Parameter	21
6.	Dimensionless Time for Complete Solidification as a Function of c/b with Biot Number as a Parameter	22
7.	Dimensionless Wall Temperature as a Function of c/b with Biot Number as a Parameter	23
8.	Frozen Fraction and Dimensionless Wall Temperature as a Function of Time for Oblate Spheroidal Coordinates	28
9.	Frozen Fraction and Dimensionless Wall Temperature as a Function of Time for Prolate Spheroidal Coordinates	32
10.	Bicylindrical Coordinates	33
11.	Percent Error in $SteFo$ due to Neglecting the Sensible Heat Effect as a Function of Stefan Number with Biot Number as a Parameter	36
12.	Frozen Fraction and Dimensionless Temperature Difference as a Function of Time for Several Geometries	39

TABLES

1.	Flux Boundary Condition Equations	40
2.	Comparison of Eqs. (38) and (39) with the Numerical Results of Ref. 12 for Biot = 1.0	42

I. INTRODUCTION

Problems involving solidification or melting of materials are of considerable importance in many technical fields such as casting processes, food freezing, crystal growing, cryosurgery, thermal energy storage, and satellite temperature control applications, to mention a few. Heat conduction problems involving freezing or melting are complicated due to the coupling of the temperature field with the rate of propagation of the phase boundary between the solid and liquid phases. Only a few exact analytical solutions have been found, e.g., Neumann's solution to the one-dimensional Cartesian case reported in Carslaw and Jaeger.¹ Most available solutions are obtained by analytical approximations and numerical methods. The one-dimensional problem for simple shapes such as plates, cylinders, and spheres has been treated by various analytical techniques, e.g., the heat balance integral method by Goodman,² the variational method by Biot,³ the method of moving heat sources by Rosenthal⁴ and the method of polynomial approximation by Megerlin⁵ and Lin.⁶ London and Seban⁷ obtained exact closed-form solutions by assuming that the heat capacity of the solidified or melted substance is negligible relative to the latent heat of fusion. This assumption greatly

¹ Carslaw, H.S., and Jaeger, J.C., Conduction of Heat in Solids, 2nd ed., Oxford University Press, London and New York, 1959.

² Goodman, T.R., "The Heat-Balance Integral and Its Application to Problems Involving a Change of Phase," Transactions of ASME, Vol. 80, 1958, pp. 335-342.

³ Biot, M.A., and Daughaday, H., "Variational Analysis of Ablation," Journal of Aerospace Sciences, Vol. 29, No. 2, 1962, pp. 227-228.

⁴ Rosenthal, D., "The Theory of Moving Sources of Heat and Its Application to Metal Treatments," Transactions of ASME, Vol. 68, 1946, pp. 849-866.

⁵ Megerlin, F., "Geometrisch eindimensionale Wärmeleitung beim Schmelzen und Erstarren," Forsch. Ing.-Wes., Vol. 34, 1968, pp. 40-46.

⁶ Lin, S., "An Analytical Method for Solving Geometric One-dimensional Freezing or Melting Problems," ASME Paper No. 73-WA/HT-33.

⁷ London, A.L., and Seban, R.A., "Rate of Ice Formation," Transactions of the ASME, Vol. 6, 1943, pp. 771-778.

simplifies the mathematics but limits the applicability of the solution to a certain class of problems as discussed below. Numerical solutions to the one-dimensional phase-change problems for simple shapes such as slabs, cylinders, and spheres are too numerous to mention here. References 8 and 9 are good starting points.

Multidimensional phase-change problems are very complex to solve analytically even for highly idealized situations such as those treated in Refs. 10 and 11; the common approach is to use numerical methods.¹² However, several seemingly multidimensional problems can be closely approximated by one-dimensional techniques if a proper coordinate system is used so that the physical boundaries of the system can be made to coincide with the coordinate surfaces.^{13, 14} The purpose of this report is to develop a unified approach in the use of orthogonal curvilinear coordinates to conduct problems involving phase-change and to present examples in several of the most common coordinate systems. The closed-form expressions obtained give the solidified (or melted) fraction, interface position, boundary temperatures, and heat fluxes as a function of time for elliptic cylinder and spheroidal phase-change containers of various eccentricities.

⁸Ehrlich, L. W., "A Numerical Method of Solving a Heat Flow Problem with Moving Boundary," Journal of ACM, Vol. 5, 1958, pp. 161-176.

⁹Murray, W. D., and Landis, F., "Numerical and Machine Solutions of Transient Heat-Conduction Problems Involving Melting or Freezing," Transaction of ASME, Vol. 81, 1959, pp. 106-112.

¹⁰Poots, G., "An Approximate Treatment of Heat Conduction Problem Involving a Two-Dimensional Solidification Front," International Journal of Heat and Mass Transfer, Vol. 5, 1962, pp. 339-348.

¹¹Rathjen, K. A., and Jiji, L. M., "Heat Conduction with Melting or Freezing in a Corner," Journal of Heat Transfer, Trans. ASME, Series C, Vol. 93, 1971, pp. 101-109.

¹²Shamsundar, N., and Sparrow, E. M., "Analysis of Multidimensional Conduction Phase Change Via the Enthalpy Model," Journal of Heat Transfer, Trans. ASME, Series C, Vol. 97, 1975, pp. 333-340.

¹³Yovanovich, M. M., Advanced Heat Conduction, Hemisphere Publishing Corporation, Washington, D. C., 1978.

¹⁴Moon, P., and Spencer, D. E., Field Theory for Engineers, D. Van Nostrand Company, Inc., Princeton, New Jersey, 1961.

II. ANALYSIS

A. CARTESIAN COORDINATES

Consider first the relatively straightforward case of idealized freezing between two infinite parallel plates as shown in Fig. 1a. At time $t = 0$ the content between parallel plates is assumed to be a pure liquid at its freezing or melting temperature. As the outer walls are cooled by contact with another medium at T_o , the solidification boundary moves inward toward smaller values of x . The effects of supercooling, density changes due to change of phase, convection between the two phases, and temperature drop through the container wall are neglected. Let Q be the heat rate removed from the surface at x_o through a heat transfer coefficient h_o . If the sensible thermal energy stored in the solidified layer is small compared to the latent-heat-of-freezing, heat flowing from the solid-liquid interface at x is also equal to Q and is given by

$$Q = \frac{T_{fr} - T_o}{\frac{1}{h_o A_o} + \frac{x_o - x}{kA}} \quad (1)$$

This heat flow provides extraction of the latent heat of fusion necessary for freezing at the surface x

$$Q = L \frac{d}{dt} (x_o - x) A \rho \quad (2)$$

where $(d/dt)(x_o - x)A\rho$ is the mass rate of solidification at the growing surface kg/s, and L is the latent heat of fusion cal/gm. When Eqs. (1) and (2) are equated to eliminate Q

$$\frac{T_{fr} - T_o}{\rho L} dt = - \left(\frac{1}{h_o} + \frac{x_o - x}{k} \right) dx \quad (3)$$

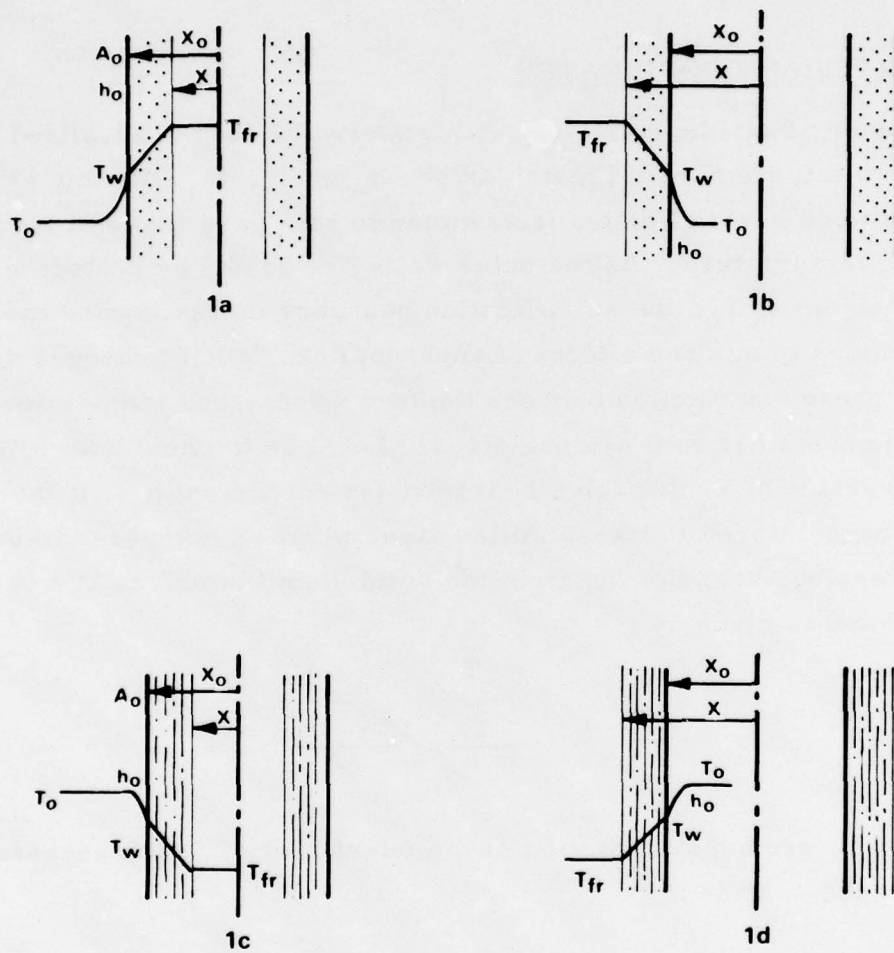


Fig. 1. Idealized Temperature Distributions during Phase Change

where $A = A_o$ for Cartesian coordinates. Equation (3) can be readily non-dimensionalized by employing the dimensionless distance coordinate $x^* = x/x_o \leq 1.0$ and the Biot number $Bi = h_o x_o / k$ as follows:

$$\frac{k(T_{fr} - T_o)}{\rho L x_o^2} dt = - \left[\left(\frac{1}{Bi} + 1 \right) - x^* \right] dx^* \quad (4)$$

For the case of inward solidification, Eq. (4) can be integrated from $x^* = 1$ at $t = 0$ to $x^* = x^*$ at t ; the result is

$$\frac{k(T_{fr} - T_o)t}{\rho L x_o^2} \equiv SteFo = \left(\frac{1}{Bi} + 1 \right) (1 - x^*) - \frac{1}{2} (1 - x^{*2}) \quad (5)$$

where the dimensionless time parameter is the product of the Stefan number $Ste = C(T_{fr} - T_o)/L$ times the Fourier number $Fo = (k/\rho CL^2)t$. The Stefan number is the ratio of the specific heat effect to latent heat. For heat storage applications it is sometimes more convenient to express Eq. (5) in terms of the frozen fraction F , which is defined by $F = (x_o - x)/x_o = 1 - x^*$

$$SteFo = \frac{F}{Bi} + \frac{F^2}{2} \quad (6)$$

The wall temperature history can be readily obtained by equating the heat flow through the outer surface $h_o A_o (T_w - T_o)$ to Eq. (1) and rearranging

$$\frac{T_w - T_o}{T_{fr} - T_o} = \frac{1}{1 + Bi(1 - x^*)} = \frac{1}{1 + BiF} = \frac{1}{\sqrt{1 + 2Bi^2 SteFo}} \quad (7)$$

The plotted results from Eqs. (6) and (7) will be presented later when freezing in elliptic cylinders is compared with oblate spheroids of high eccentricity. Note that the boundary condition temperature T_o in Eq. (2) could be a function of time without complicating the integration significantly. Closed-form solutions are still obtainable, as long as the assumed function can be integrated.

Equations (6) and (7) are also applicable for the case of melting, as shown in Fig. 1c, the only difference being that in this case F is the melted fraction and $T_o > T_w > T_{fr}$. The case of freezing in an outward direction, Fig. 1b, can also be similarly derived by equating the heat extraction rate to the mass rate of freezing

$$\frac{T_{fr} - T_o}{\frac{1}{h_o A} + \frac{x - x_o}{kA}} = \rho AL \frac{dx}{dt} \quad (8)$$

Using the same nondimensional terms as before and integrating from $x^* = 1$ at $t = 0$ to $x^* = x^*$ at t results in

$$SteFo = \left(\frac{1}{Bi} - 1 \right) \left(x^* - 1 \right) + \frac{1}{2} \left(x^{*2} - 1 \right) \quad (9)$$

where $x^* = x/x_o \geq 1.0$. This equation is valid for outward freezing or melting (see Figs. 1b and 1d).

B. GENERALIZED COORDINATES

Before proceeding with formulation of the problem in general curvilinear coordinates, a general expression for the thermal resistance, comparable to the x/kA for Cartesian coordinates, is required. Special coordinate systems are used because it is sometimes possible to make the isothermal surfaces of a given heat conduction problem coincident with coordinate surfaces, thus making the temperature field one-dimensional in that coordinate system, e.g., the field between two concentric cylinders in circular cylinder coordinates.

Consider the orthogonal curvilinear coordinates shown in Fig. 2. The general line element ds is the diagonal of the infinitesimal parallelepiped with faces that coincide with the planes u_1 , u_2 , or $u_3 = \text{const}$ and is given by

$$ds^2 = g_1 du_1^2 + g_2 du_2^2 + g_3 du_3^2 \quad (10)$$

which can be considered as the definition of the metric coefficients g_1, g_2, g_3 that may be functions of u_1, u_2 , and u_3 . When the Cartesian coordinates x, y, z can be expressed in terms of the new coordinates, u_1, u_2, u_3 by the equations $x = x(u_1, u_2, u_3)$, $y = y(u_1, u_2, u_3)$, and $z = z(u_1, u_2, u_3)$, the metric coefficients can be readily generated by means of the following formula:^{13, 14}

$$g_i = \left(\frac{\partial x}{\partial u_i} \right)^2 + \left(\frac{\partial y}{\partial u_i} \right)^2 + \left(\frac{\partial z}{\partial u_i} \right)^2 \quad i = 1, 2, 3 \quad (11)$$

The infinitesimal volume is given by

$$dV = \sqrt{g} du_1 du_2 du_3 \quad (12)$$

where $\sqrt{g} = \sqrt{g_1 g_2 g_3}$. The elemental surface area orthogonal to the u_1 -direction is

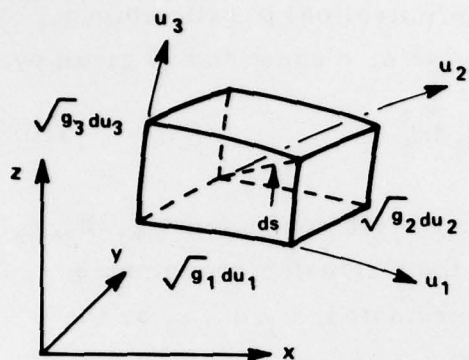
$$dA_1 = \sqrt{g_2 g_3} du_2 du_3 \quad (13)$$

Similar expressions can be written for the areas in the u_2 - and u_3 -directions. The heat flow/unit time through this surface into the volume element is

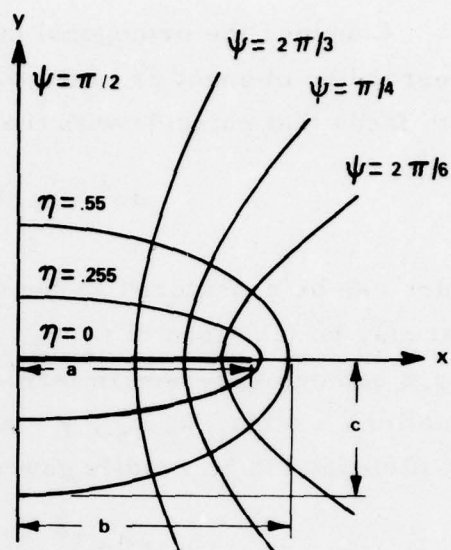
$$dQ_1 = -k dA_1 \frac{dT}{ds_1} = -k \frac{\sqrt{g}}{g_1} \frac{dT}{du_1} du_2 du_3 \quad (14)$$

The net rate of heat conduction out of the volume element is

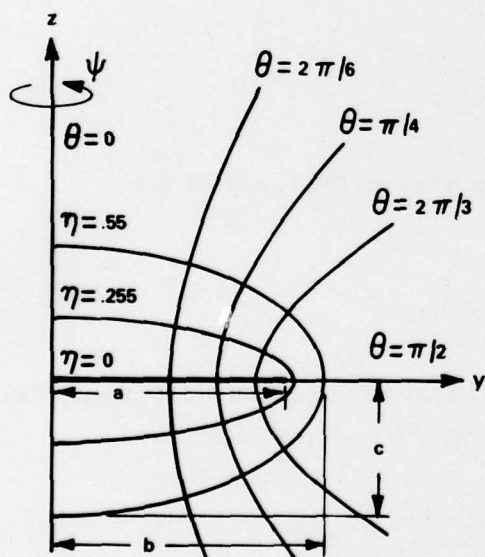
$$\frac{d}{du_1} \left(k \frac{\sqrt{g}}{g_1} \frac{dT}{du_1} \right) du_1 du_2 du_3 \quad (15)$$



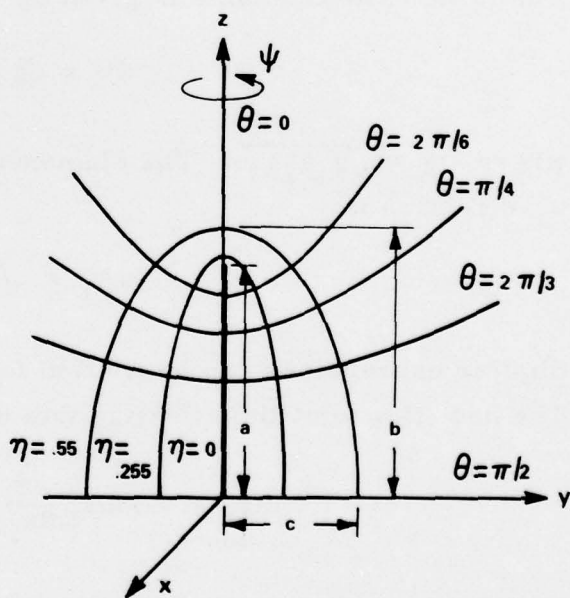
INFINITESIMAL VOLUME



ELLIPTIC CYLINDER



OBLATE SPHEROID



PROLATE SPHEROID

Fig. 2. Orthogonal Curvilinear Coordinates

Dividing by volume element $dV = \sqrt{g} du_1 du_2 du_3$ and equating to zero results in Laplace's equation in the u_1 direction

$$\frac{1}{\sqrt{g}} \frac{d}{du_1} \left(k \frac{\sqrt{g}}{g_1} \frac{dT}{du_1} \right) = 0 \quad (16)$$

Integrating once, the result is

$$k \frac{\sqrt{g}}{g_1} \frac{dT}{du_1} = C_1 \quad (17)$$

At this point the thermal conductivity is assumed to be constant and the boundary conditions are taken as

$$\begin{aligned} T &= T_1 & u_1 &= a \\ T &= T_2 & u_1 &= b \end{aligned} \quad (18)$$

Integrating Eq. (17) between these limits and solving for C_1 results in

$$C_1 = \frac{k(T_2 - T_1)}{\int_a^b \frac{g_1}{\sqrt{g}} du_1} \quad (19)$$

Substituting in Eq. (17) and solving for the temperature gradient results in

$$\frac{dT}{du_1} = \frac{T_2 - T_1}{\int_a^b \frac{g_1}{\sqrt{g}} du_1} \frac{g_1}{\sqrt{g}} \quad (20)$$

The heat flow/unit time along the u_1 -direction can be obtained by substituting in Eq. (14) and integrating between appropriate limits along u_2 and u_3

$$Q_1 = k(T_1 - T_2) \int_{u_2} \int_{u_3} \frac{du_2 du_3}{\int_a^b \frac{g_1}{\sqrt{g}} du_1} \quad (21)$$

The thermal resistance R is defined as the temperature drop over the total heat flow rate; thus

$$R^{-1} = k \int_{u_2} \int_{u_3} \frac{du_2 du_3}{\int_a^b \frac{g_1}{\sqrt{g}} du_1} \quad (22)$$

Yovanovich^{13, 15} derived this equation for the more general case of thermal conductivity as a linear function of temperature and showed that Eq. (22) is valid if k represents the arithmetic average conductivity. He also specialized Eq. (22) for the most frequently used coordinate systems.¹⁵

Consider a phase-change material (PCM) confined between two isothermal surfaces of a general orthogonal coordinate system at different temperature levels with phase change taking place inwardly from a larger outer surface to a smaller inner surface. A heat balance similar to Eq. (3) for the Cartesian coordinate case can be written as follows:

$$\frac{\Delta T}{\frac{h_o A_o}{h_o A_o} + \left(k \int_{u_j} \int_{u_k} \frac{du_j du_k}{\int_a^b \frac{g_i}{\sqrt{g}} du_1} \right)^{-1}} = \rho L \frac{d}{dt} (V_o - V) \quad (23)$$

where all assumptions made in deriving Eq. (3) apply for this equation as well. When phase change proceeds in an outward direction, from the smaller area toward a larger area, the right-hand side of the equation is changed to $\rho L dV/dt$. Equation (23) will be specialized and solved for elliptic cylinder, oblate spheroidal, prolate spheroidal, and bicylindrical coordinates.

¹⁵Yovanovich, M.M., "A General Expression for Predicting Conduction Shape Factors," AIAA Paper No. 73-121.

C. ELLIPTIC CYLINDER COORDINATES (η, θ, z)

Phase change conduction problems in or around elliptic cylinders can be enormously simplified by using elliptic cylinder coordinates as shown in Fig. 2. The coordinates are obtained by taking an orthogonal family of confocal ellipses and hyperbolas in a plane and translating them in the z -direction. The coordinate surfaces of interest here are elliptic cylinders ($\eta = \text{const}$). The relations between the elliptic and Cartesian coordinates are

$$\begin{aligned}x &= a \cosh \eta \cos \psi \\y &= a \sinh \eta \sin \psi \\z &= z\end{aligned}\tag{24}$$

The metric coefficients can be easily derived by the use of Eq. (11)

$$g_{\eta} = g_{\psi} = a^2 \cosh^2 \eta - \cos^2 \psi, \quad g_z = 1\tag{25}$$

From Eq. (24) it can be seen that $b = a \cosh \eta$, $c = a \sinh \eta$ and $\eta = \tanh^{-1} c/b$. The thermal resistance between two elliptic cylinders is readily obtained by Eq. (22) or taken directly from Refs. 13 or 15.

$$R = \frac{\eta_o - \eta}{2\pi \ell k}\tag{26}$$

The heat balance equation is

$$\frac{T_{fr} - T_o}{\frac{1}{h_o A_o} + \frac{\eta_o - \eta}{2\pi \ell k}} = \rho L \frac{d}{dt} (V_o - V) = - \rho L \frac{dV}{dt}\tag{27}$$

The area A_o can be computed from Eq. (13) as follows:

$$A_o = \int_0^{\ell} \int_0^{2\pi} \sqrt{g_{\psi} g_z} d\psi dz = 4 \int_0^{\ell} \int_0^{\pi/2} a \sqrt{\cosh^2 \eta - \cos^2 \psi} d\psi dz\tag{28}$$

Letting $\psi = 90 - \phi$, it can be shown that

$$A_o = 4a\ell \cosh\eta_o E(\eta_o) \quad (29)$$

where $E(\eta_o)$ is the complete elliptic integral of the first kind tabulated in most mathematical tables and shown in Fig. 3 for ease of reference. The expression for the volume V can be calculated from Eq. (12) by triple integration.

$$V = 4a^2 \int_0^{\ell} \int_0^{\pi/2} \int_0^{\eta} (\cosh^2\eta - \cos^2\psi) d\eta d\psi dz = \frac{\pi}{2} a^2 \ell \sinh 2\eta \quad (30)$$

Differentiating with respect to time and substituting the heat balance equation becomes

$$\frac{k(T_{fr} - T_o)}{\rho L a^2} dt = - \left[\frac{k}{4a\ell h_o \cosh\eta_o E(\eta_o)} + \frac{\eta_o - \eta}{2\pi\ell} \right] \pi\ell \cosh 2\eta d\eta \quad (31)$$

For the case of inward solidification, the limits of integration are from $\eta = \eta_o$ at $t = 0$ to $\eta = \eta$ at $t = t$

$$\begin{aligned} \frac{k(T_{fr} - T_o)t}{\rho L c^2} = & \left\{ \frac{\pi \sqrt{\left(\frac{b}{c}\right)^2 - 1}}{4Bi \cosh\eta_o E(\eta_o)} + \frac{\eta_o}{2} \left[\left(\frac{b}{c}\right)^2 - 1 \right] \right\} \\ & \cdot \int_{\eta}^{\eta_o} \cosh 2\eta d\eta - \left[\left(\frac{b}{c}\right)^2 - 1 \right] \int_{\eta}^{\eta_o} \frac{\eta}{2} \cosh 2\eta d\eta \end{aligned} \quad (32)$$

where the semiminor axis c has been used to define the Biot number $Bi = h_o c/k$. The term on the left-hand side of the equation is the product of the Stefan and Fourier numbers. Performing the integrations shown finally results in

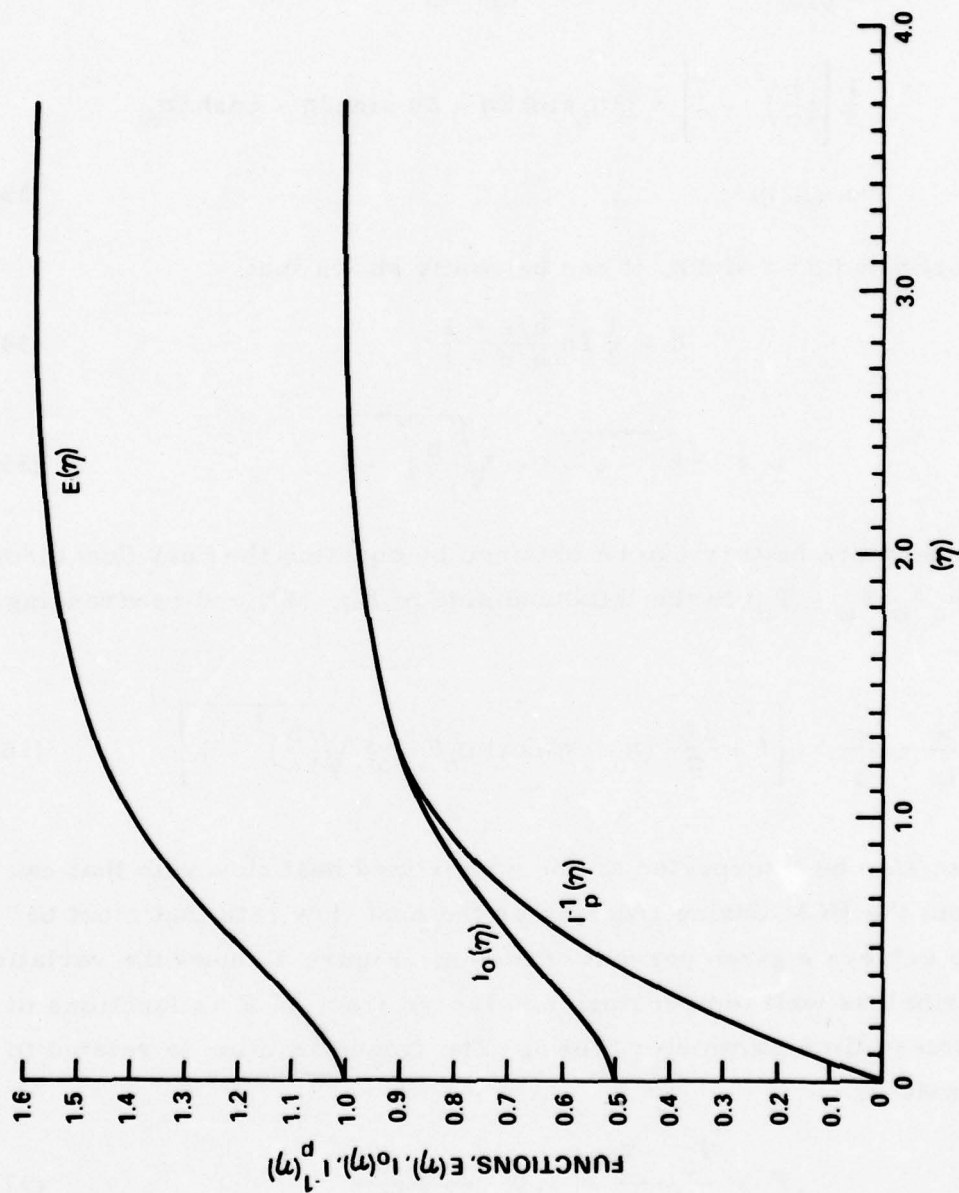


Fig. 3. Special Functions $E(\eta)$, $I_0(\eta)$ and $I_p^{-1}(\eta)$ to Facilitate the Computation of the Elliptic Cylinder, Oblate Spheroidal and Prolate Spheroidal Results, Respectively

$$\begin{aligned}
SteFo = \frac{k(T_{fr} - T_o)t}{\rho Lc^2} &= \frac{\pi \sqrt{\left(\frac{b}{c}\right)^2 - 1}}{8Bi \cosh \eta_o E(\eta_o)} (\sinh 2\eta_o - \sinh 2\eta) \\
&- \frac{1}{8} \left[\left(\frac{b}{c}\right)^2 - 1 \right] \cdot (2\eta_o \sinh 2\eta - 2\eta \sinh 2\eta - \cosh 2\eta_o \\
&+ \cosh 2\eta)
\end{aligned} \tag{33}$$

Since $b = a \cosh \eta$ and $c = a \sinh \eta$, it can be easily shown that

$$\eta = \frac{1}{2} \ln \frac{b/c + 1}{b/c - 1} \tag{34}$$

$$a = \sqrt{b^2 - c^2} = c \sqrt{\left(\frac{b}{c}\right)^2 - 1} \tag{35}$$

The wall temperature history can be obtained by equating the heat flow through the surface $h_o A_o (T_w - T_o)$ to the left-hand side of Eq. (27) and rearranging; the result is

$$\frac{T_w - T_o}{T_{fr} - T_o} = \left[1 + \frac{2Bi}{\pi} (\eta_o - \eta) \cosh \eta_o E(\eta_o) \sqrt{\left(\frac{b}{c}\right)^2 - 1} \right]^{-1} \tag{36}$$

This ratio can also be interpreted as the normalized heat flow rate that can be extracted from the PCM during freezing or the heat flow rate that must be introduced to achieve a given percent of fusion. Figure 4 shows the variation of the dimensionless wall temperature and frozen fraction F as functions of the dimensionless time parameter $SteFo$. The frozen fraction is related to the η -coordinate by

$$F = \frac{V_o - V}{V_o} = 1.0 - \frac{\sinh 2\eta}{\sinh 2\eta_o} \tag{37}$$

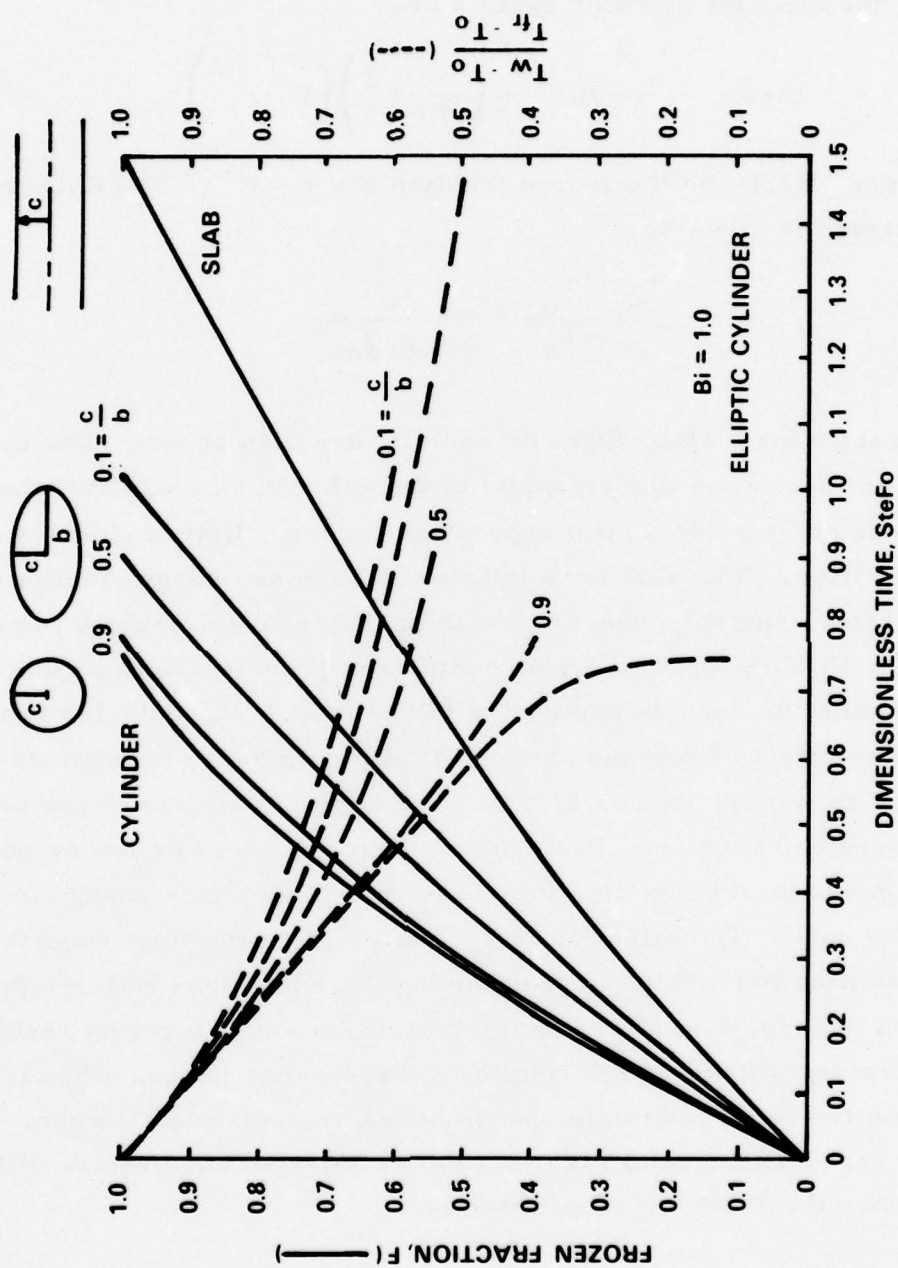


Fig. 4. Frozen Fraction and Dimensionless Wall Temperature as a Function of Time for Elliptic Coordinates

As c/b approaches unity, the results approach the limiting case of a circular cylinder derived by London and Seban.⁷ In terms of the symbols used in this report, the circular cylinder results are

$$\text{SteFo} = \frac{r^{*2}}{2} \ln r^* + \left(\frac{1}{2\text{Bi}} + \frac{1}{4} \right) (1 - r^{*2}) \quad (38)$$

where $r^* = r/r_o \leq 1.0$ and the frozen fraction $F = 1 - r^{*2}$. The dimensionless wall temperature is given by

$$\frac{T_w - T_o}{T_{fr} - T_o} = \frac{1}{1 - \text{Bi} \ln r^*} \quad (39)$$

The results for a slab, Eqs. (6) and (7), are also shown. The case for $c/b = 0.01$, not shown, is closely equal to the $c/b = 0.1$ case; thus, the slab results do not provide a good approximation for elliptic cylinders of high eccentricities. Note that for applications such as energy storage or close temperature control, where a low temperature difference is required throughout the PCM, elliptic cylinder containers provide a better choice than circular cylinders as seen by comparing the $c/b = 0.9$ and cylinder results in Fig. 4. The effect of Biot number on elliptic cylinders of moderate eccentricities is summarized in Fig. 5. For applications where low temperature differences are required, Biot number should be kept as low as possible within the constraint of being able to achieve complete phase change in the allocated time span. The effect of eccentricity c/b on the time required for complete solidification and the corresponding dimensionless wall temperature is shown in Figs. 6 and 7. Low Biot numbers and c/b ratios result in small temperature differences during the phase-change process; however, the corresponding times for complete phase change are relatively larger. When the Biot number is sufficiently high, a relatively large temperature difference develops across the PCM for all c/b values.

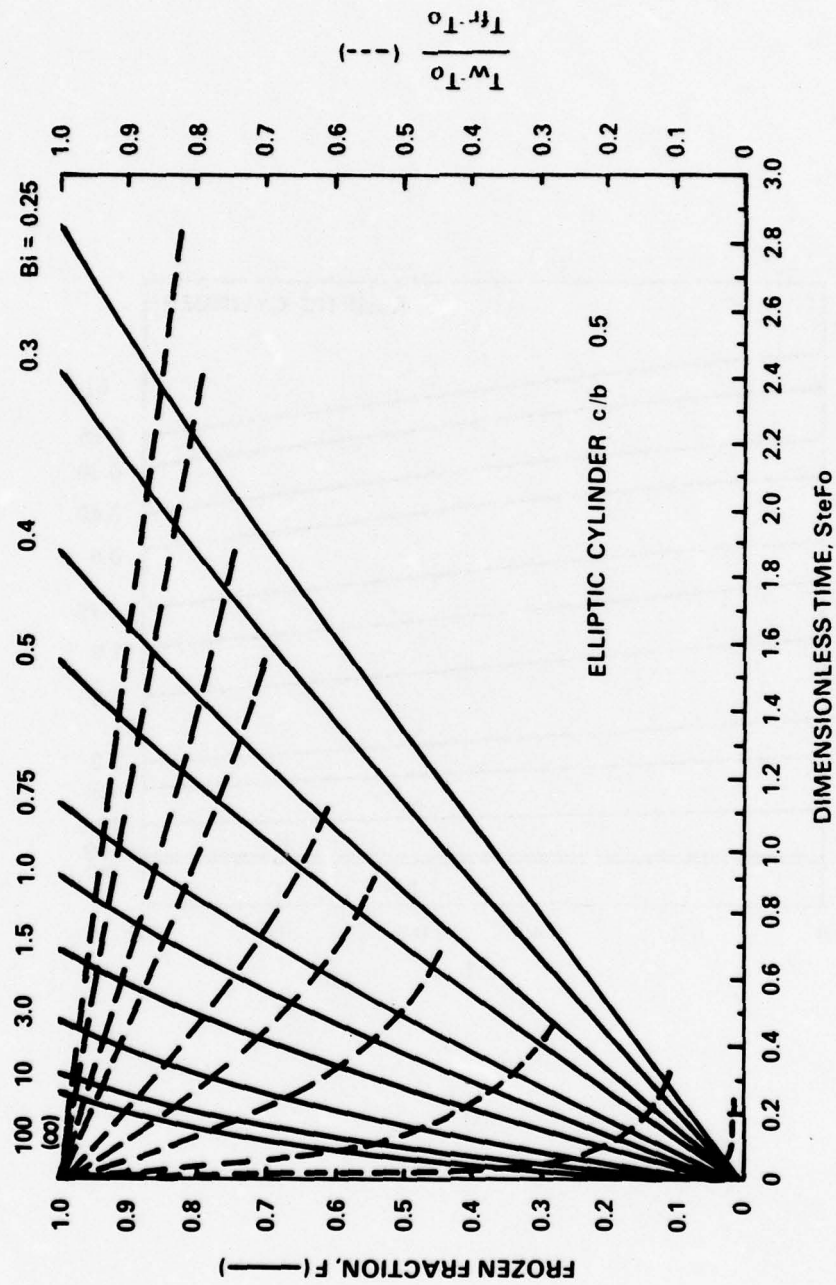


Fig. 5. Frozen Fraction and Dimensionless Wall Temperature as a Function of Time with Biot Number as a Parameter

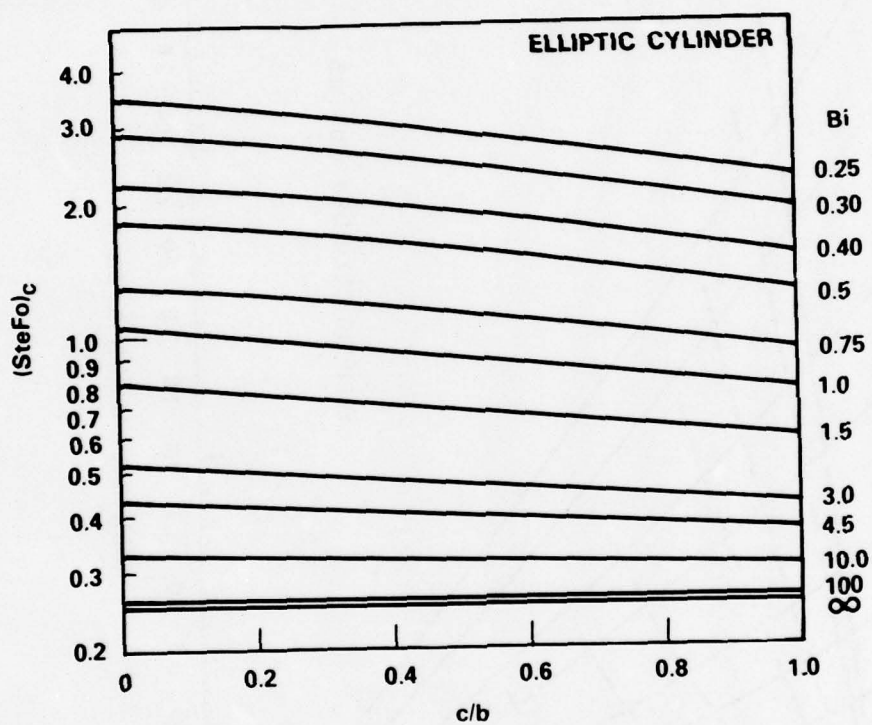


Fig. 6. Dimensionless Time for Complete Solidification as a Function of c/b with Biot Number as a Parameter

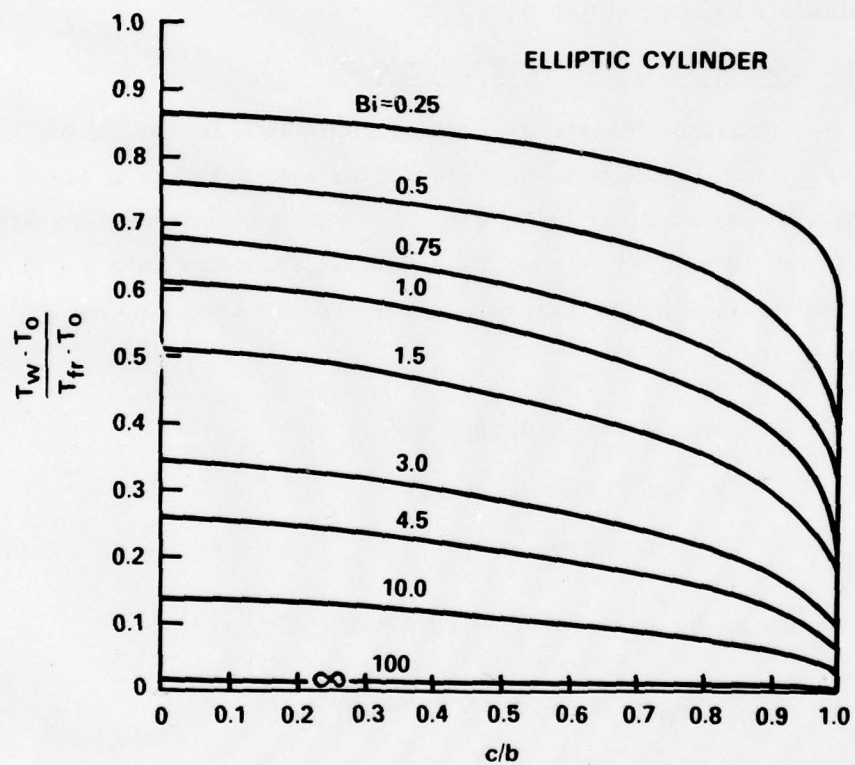


Fig. 7. Dimensionless Wall Temperature as a Function of c/b with Biot Number as a Parameter

For phase-change problems in an outward direction where $\eta > \eta_0$, it can be shown that the dimensionless time to reach a given position η is obtained by placing a negative sign on the first term only of Eq. (33). The wall temperature of the inner boundary T_w can be calculated from Eq. (36) if $(\eta_0 - \eta)$ is changed to $(\eta - \eta_0)$. The resulting expression can be used to estimate the rate at which a phase-change front would move into the half-space above the x-axis from a strip of length $2a$ located on the x-axis, which is assumed to be insulated everywhere else.

D. OBLATE SPHEROIDAL COORDINATES (η, θ, ψ)

The oblate spheroidal coordinate system is generated by taking an orthogonal family of confocal ellipses and hyperbolas and rotating it about the minor axis of the ellipses as shown in Fig. 2. The $\eta = \text{const}$ solids are called oblate spheroids. When $\eta = 0$, the spheroid degenerates into a flat disk of radius a . The relations between oblate spheroidal coordinates and Cartesian coordinates are¹³

$$\begin{aligned} x &= a \cosh \eta \sin \theta \cos \psi \\ y &= a \cosh \eta \sin \theta \sin \psi \\ z &= a \sinh \eta \cos \theta \end{aligned} \quad (40)$$

The metric coefficients can be easily derived by using Eq. (11)

$$\begin{aligned} g_\eta &= g_\theta = a^2 (\cosh^2 \eta - \sin^2 \theta) \\ g_\psi &= a^2 \cosh^2 \eta \sin^2 \theta \end{aligned} \quad (41)$$

From Eq. (40) the semimajor axis is $b = a \cosh \eta$ and the semiminor axis is $c = a \sinh \eta$ from which $\eta = \tanh^{-1} c/b$.

The thermal resistance between two oblate spheroids can be obtained by performing the integrations indicated in Eq. (22) or by using the results of Ref. 15 directly

$$R = \frac{\tan^{-1}(\sinh \eta_o) - \tan^{-1}(\sinh \eta)}{4\pi ka} \quad (42)$$

where $\eta < \eta_o$ for the inward solidification case. The heat balance equation can now be written as before

$$\frac{T_{fr} - T_o}{\frac{h_o A_o}{4\pi ka} + \frac{\tan^{-1}(\sinh \eta_o) - \tan^{-1}(\sinh \eta)}{4\pi ka}} = - \rho L \frac{dV}{dt} \quad (43)$$

The area A_o can be computed from Eq. (13)

$$\begin{aligned} A_o &= 4\pi a^2 \cosh^2 \eta_o \int_0^{\pi/2} \sin \theta \sqrt{1 - \left(\frac{1}{\cosh^2 \eta_o} \right) \sin^2 \theta} d\theta \\ &= 4\pi a^2 \cosh^2 \eta_o I_o(\eta_o) \end{aligned} \quad (44)$$

where the definite integral $I_o(\eta)$ is plotted in Fig. 3. Volume V can be found by integrating Eq. (12)

$$V = \frac{4\pi a^3}{3} (\sinh \eta + \sinh^3 \eta) \quad (45)$$

Differentiating with respect to time and substituting in Eq. (43) above, together with Eq. (44), gives

$$\begin{aligned}
\frac{k(T_{fr} - T_o)t}{\rho L c^2} = & \left\{ \left(\frac{1}{Bi} \right) \frac{\sqrt{\left(\frac{b}{c} \right)^2 - 1}}{\cosh^2 \eta_o I_o(\eta_o)} + \left[\left(\frac{b}{c} \right)^2 - 1 \right] \tan^{-1}(\sinh \eta_o) \right\} \cdot \int_{\eta}^{\eta_o} (\cosh^3 \eta \\
& - \frac{2}{3} \cosh \eta) d\eta - \left[\left(\frac{b}{c} \right)^2 - 1 \right] \cdot \int_{\eta}^{\eta_o} \tan^{-1}(\sinh \eta) \\
& \cdot \left[\cosh^3 \eta - \frac{2}{3} \cosh \eta \right] d\eta
\end{aligned} \tag{46}$$

The integrations shown on the right-hand side of the equation can be carried out in closed form with the following final result:

$$\begin{aligned}
SteFo = & \left\{ \left(\frac{1}{Bi} \right) \frac{\sqrt{\left(\frac{b}{c} \right)^2 - 1}}{\cosh^2 \eta_o I_o(\eta_o)} + \left[\left(\frac{b}{c} \right)^2 - 1 \right] \tan^{-1}(\sinh \eta_o) \right\} \cdot I_1 \\
& - \left[\left(\frac{b}{c} \right)^2 - 1 \right] I_2
\end{aligned} \tag{47}$$

where

$$\begin{aligned}
I_1 &= \frac{1}{12} (\sinh 3\eta_o + \sinh \eta_o - \sinh 3\eta - \sinh \eta) \\
I_2 &= \frac{1}{12} \left[(\sinh 3\eta_o + \sinh \eta_o) \tan^{-1}(\sinh \eta_o) \right. \\
&\quad \left. - (\sinh 3\eta + \sinh \eta) \cdot \tan^{-1}(\sinh \eta) \right] \\
&\quad - \frac{1}{12} (\cosh 2\eta_o - \cosh 2\eta)
\end{aligned}$$

As in the elliptic cylinder case, the Biot number is defined in terms of the semiminor axis c which is related to a by $a = \sqrt{b^2 - c^2}$.

The wall temperature history can be obtained by equating the heat flow through the outer surface $h_o A_o (T_w - T_o)$ to the left-hand side of Eq. (43) and rearranging; the result is

$$\frac{T_w - T_o}{T_{fr} - T_o} = \left\{ 1 + Bi \cosh^2 \eta_o I_o(\eta_o) \left[\tan^{-1}(\sinh \eta_o) - \tan^{-1}(\sinh \eta) \right] \cdot \sqrt{\left(\frac{b}{c}\right)^2 - 1} \right\}^{-1} \quad (48)$$

Figure 8 shows Eqs. (47) and (48) plotted for $Bi = 1.0$ for oblate spheroids of c/b ratios of 0.9, 0.5, and 0.1. The frozen fraction F is related to the η -coordinate by

$$F = \frac{V_o - V}{V_o} = 1.0 - \frac{\sinh \eta \cosh^2 \eta}{\sinh \eta_o \cosh^2 \eta_o} \quad (49)$$

As c/b approaches unity, the results approach the limiting case of a sphere derived in Ref. 7. In terms of the symbols used herein, the sphere results are

$$SteFo = \frac{1}{3} \left(\frac{1}{Bi} - 1 \right) \left(1 - r^{*3} \right) + \frac{1}{2} \left(1 - r^{*2} \right) \quad (50)$$

where $r^* = r/r_o \leq 1.0$ and the frozen fraction $F = 1 - r^{*3}$. The dimensionless wall temperature is given by

$$\frac{T_w - T_o}{T_{fr} - T_o} = \left[1 + Bi \left(\frac{1}{r^*} - 1 \right) \right]^{-1} \quad (51)$$

The case for $c/b = 0.01$, not shown, is almost equal to the $c/b = 0.1$ case; thus the slab results do not provide a good approximation for disklike oblate spheroids of high eccentricities. For applications where a low temperature

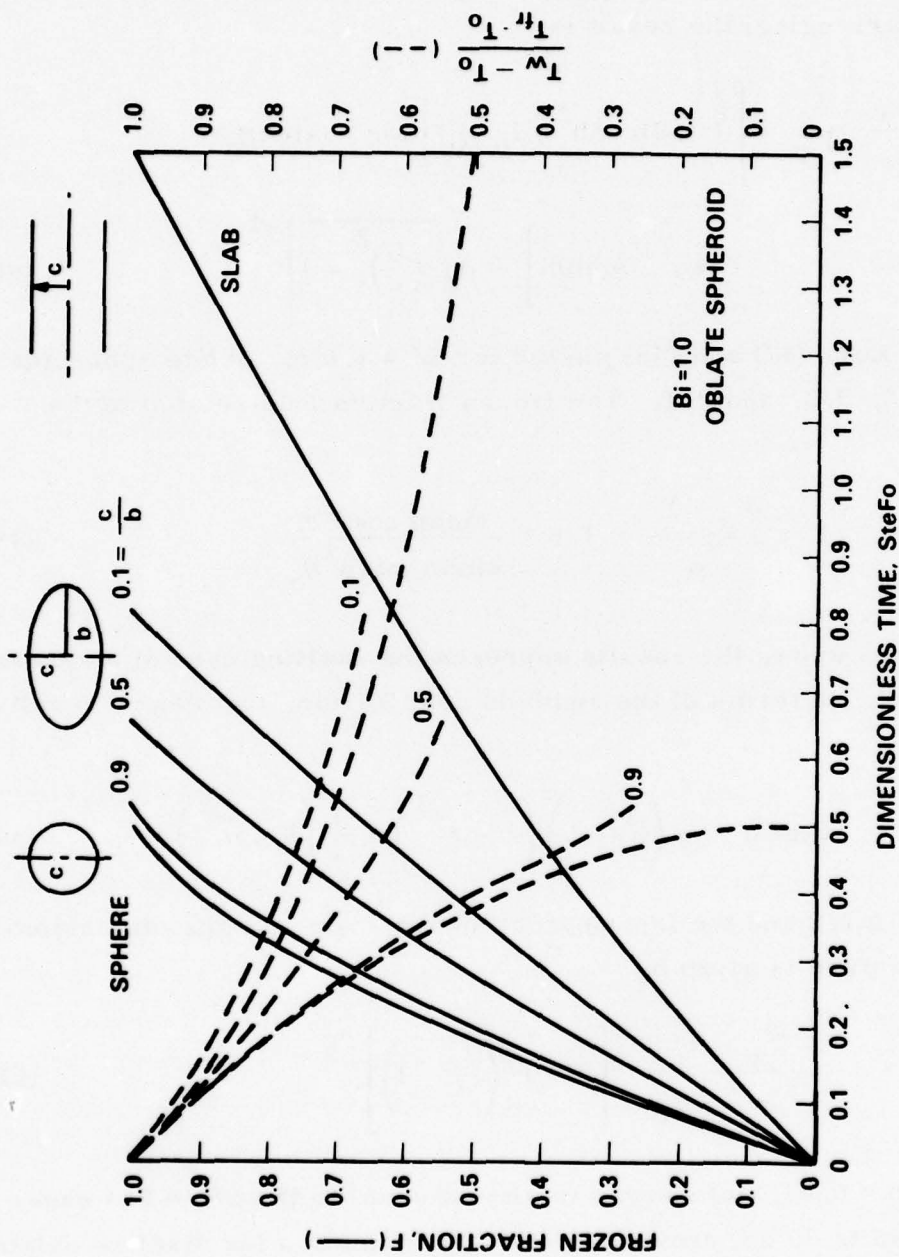


Fig. 8. Frozen Fraction and Dimensionless Wall Temperature as a Function of Time for Oblate Spheroidal Coordinates

difference is required throughout the PCM, oblate spheroidal coordinates provide a better choice than spheres. The effect of eccentricity c/b on the time required for complete solidification ($\eta = 0$) and the corresponding dimensionless wall temperature are qualitatively similar to the calculated results for the elliptic cylinder case shown in Figs. 6 and 7.

For phase-change problems in an outward direction where $\eta > \eta_0$, it can be shown that the dimensionless time to reach a given position η is obtained by placing a negative sign before the first term, inside the bracket, of Eq. (47). The wall temperature of the inner boundary T_w can be calculated from Eq. (48) by placing a negative sign in front of the second term inside the brackets. The resulting expression can be used to estimate the rate at which a phase-change point would move into the half-space above the x-axis from a circular disc of radius a , located on the x-axis, which is assumed to be insulated everywhere else.

E. PROLATE SPHEROIDAL COORDINATES (η, θ, ψ)

The prolate spheroidal coordinate system is generated by rotating an orthogonal family of confocal ellipses and hyperbolas about the major axis of the ellipses as shown in Fig. 2. The prolate spheroids, $\eta = \text{constant}$ solids, vary in shape from near-spherical to thin rods of finite length. The relations between prolate spheroidal coordinates and Cartesian coordinates are¹³

$$\begin{aligned}x &= a \sinh \eta \sin \theta \cos \psi \\y &= a \sinh \eta \sin \theta \sin \psi \\z &= a \cosh \eta \cos \theta\end{aligned}\tag{52}$$

The metric coefficients can be easily derived by using Eq. (11)

$$\begin{aligned}g_\eta &= g_\theta = a^2 (\sin^2 \eta + \sin^2 \theta) \\g_\psi &= a^2 \sin^2 \eta \sin^2 \theta\end{aligned}\tag{53}$$

The thermal resistance between two prolate spheroids can be obtained by using Eq. (22) or by using the result of Ref. 15 directly.

$$R = \frac{\ln[\tanh(\eta_o/2)] - \ln[\tanh(\eta/2)]}{4\pi ak} \quad (54)$$

where $\eta < \eta_o$ for the inward solidification case. The following derivation proceeds in a similar manner to the oblate spheroid case, namely, writing the heat balance equation and substituting the expressions for A_o and V which are functions of η only. The dimensionless form of the heat balance equation is

$$\frac{k(T_{fr} - T_o)t}{\rho L c^2} = \left\{ \left(\frac{1}{Bi} \right) \frac{\sqrt{\left(\frac{b}{c} \right)^2 - 1}}{\sinh^2 \eta_o I_p(\eta_o)} + \left[\left(\frac{b}{c} \right)^2 - 1 \right] \ln[\tanh(\eta_o/2)] \right\} I_1 - \left[\left(\frac{b}{c} \right)^2 - 1 \right] I_2 \quad (55)$$

where I_1 and I_2 are two integrals that can be integrated in closed form as shown below:

$$I_1 = \int_{\eta}^{\eta_o} \left(\sinh^3 \eta + \frac{2}{3} \sinh \eta \right) d\eta = \frac{1}{12} (\cosh 3\eta_o - \cosh 3\eta - \cosh \eta_o + \cosh \eta) \quad (56)$$

$$\begin{aligned} I_2 &= \int_{\eta}^{\eta_o} \ln[\tanh(\eta/2)] \left(\sinh^3 \eta + \frac{2}{3} \sinh \eta \right) d\eta = \\ &= \frac{1}{12} \ln[\tanh(\eta/2)] (\cosh 3\eta_o - \cosh \eta_o) \\ &\quad - \frac{1}{12} \ln[\tanh(\eta/2)] (\cosh 3\eta - \cosh \eta) \\ &\quad - \frac{1}{12} (\cosh 2\eta_o - \cosh 2\eta) \end{aligned} \quad (57)$$

The term $I_p(\eta_o)$ is a definite integral required to define the surface area of a prolate spheroid. Its reciprocal is plotted in Fig. 3 as a function of η . The Biot number is defined in terms of the semiminor axis c which is related to a by $a = \sqrt{b^2 - c^2}$.

The wall temperature can be obtained in a similar manner to the oblate spheroid case; the result is

$$\frac{T_w - T_o}{T_{fr} - T_o} = \left\{ 1 + \text{Bi} \sinh^2 \eta_o I_p(\eta_o) \sqrt{\left(\frac{b}{c}\right)^2 - 1} \cdot \left[\ln \frac{\tanh(\eta_o/2)}{\tanh(\eta/2)} \right] \right\}^{-1} \quad (58)$$

Figure 9 shows Eqs. (55) and (58) plotted for prolate spheroids of c/b ratios of 0.9, 0.5, and 0.1. The frozen fraction F is related to the η -coordinate by

$$F = \frac{V_o - V}{V_o} = 1.0 - \frac{\sinh^2 \eta \cosh \eta}{\sinh^2 \eta_o \cosh \eta_o} \quad (59)$$

Figure 9 illustrates that as c/b approaches unity, the frozen fraction and dimensionless wall temperature approach the limiting case of a sphere. For small values of c/b the limiting results are close to the $c/b = 0.1$ case and cannot be accurately estimated by the infinite cylinder results. For cases where the temperature difference between the wall and the freezing point must be kept at a low value, such as in thermal energy storage and close temperature control applications, the phase-change container shapes shown in Fig. 9 are not desirable because they all result in the maximum possible temperature difference at the end of the phase-change process. Elliptic cylinders, oblate spheroids, and other slablike geometries result in lower temperature differences for all values of the Biot number.

F. BICYLINDRICAL COORDINATES (η, ψ, z)

The bicylindrical coordinate system is generated by translating the two families of orthogonal circles in the xy -plane, shown in Fig. 10, parallel to the z -axis pointing into the paper. The circles $\eta = \text{const}$ are drawn about two poles $x = \pm a$, while the orthogonal family $\psi = \text{const}$ has its centers on

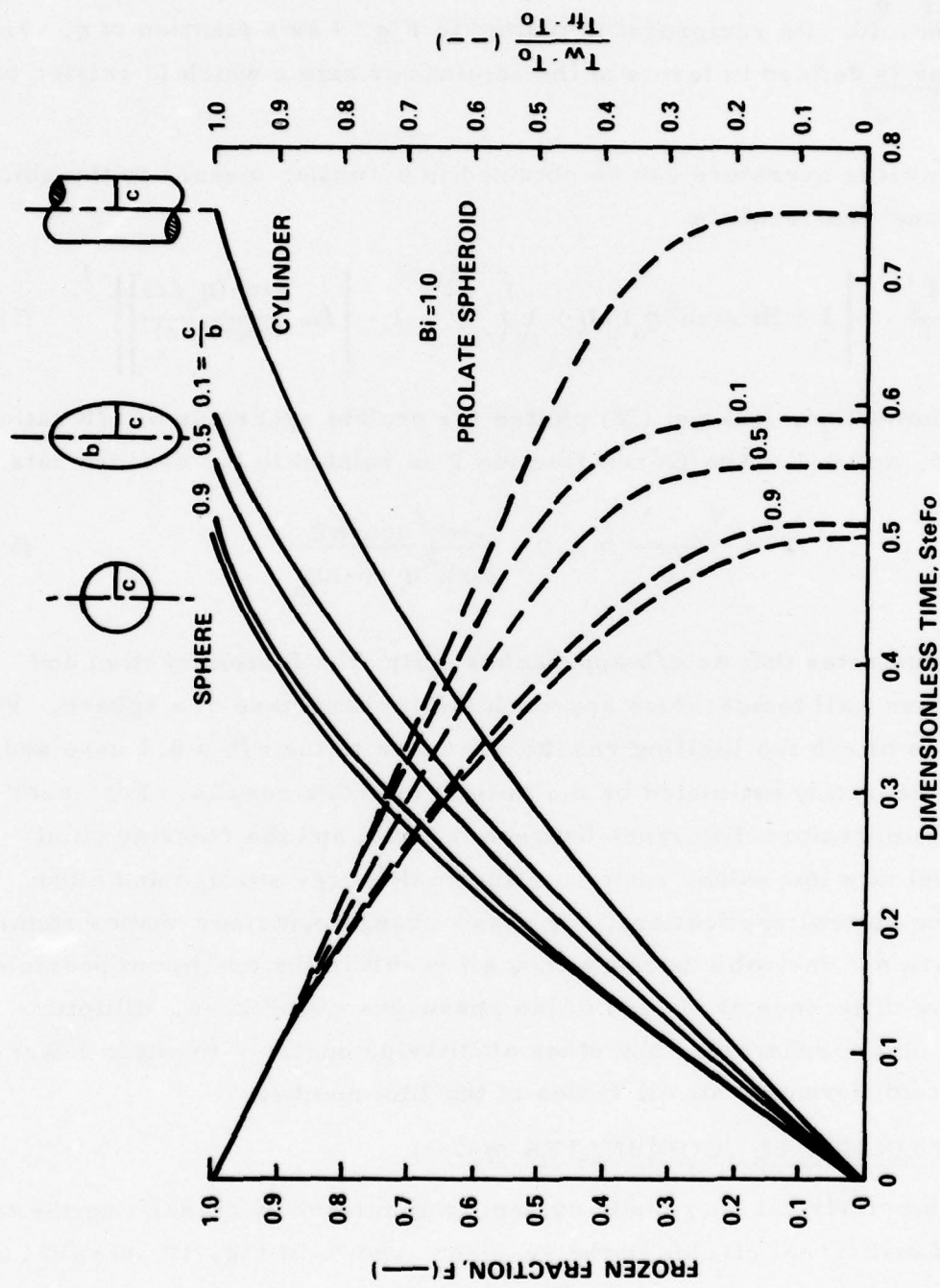


Fig. 9. Frozen Fraction and Dimensionless Wall Temperature as a Function of Time for Prolate Spheroidal Coordinates

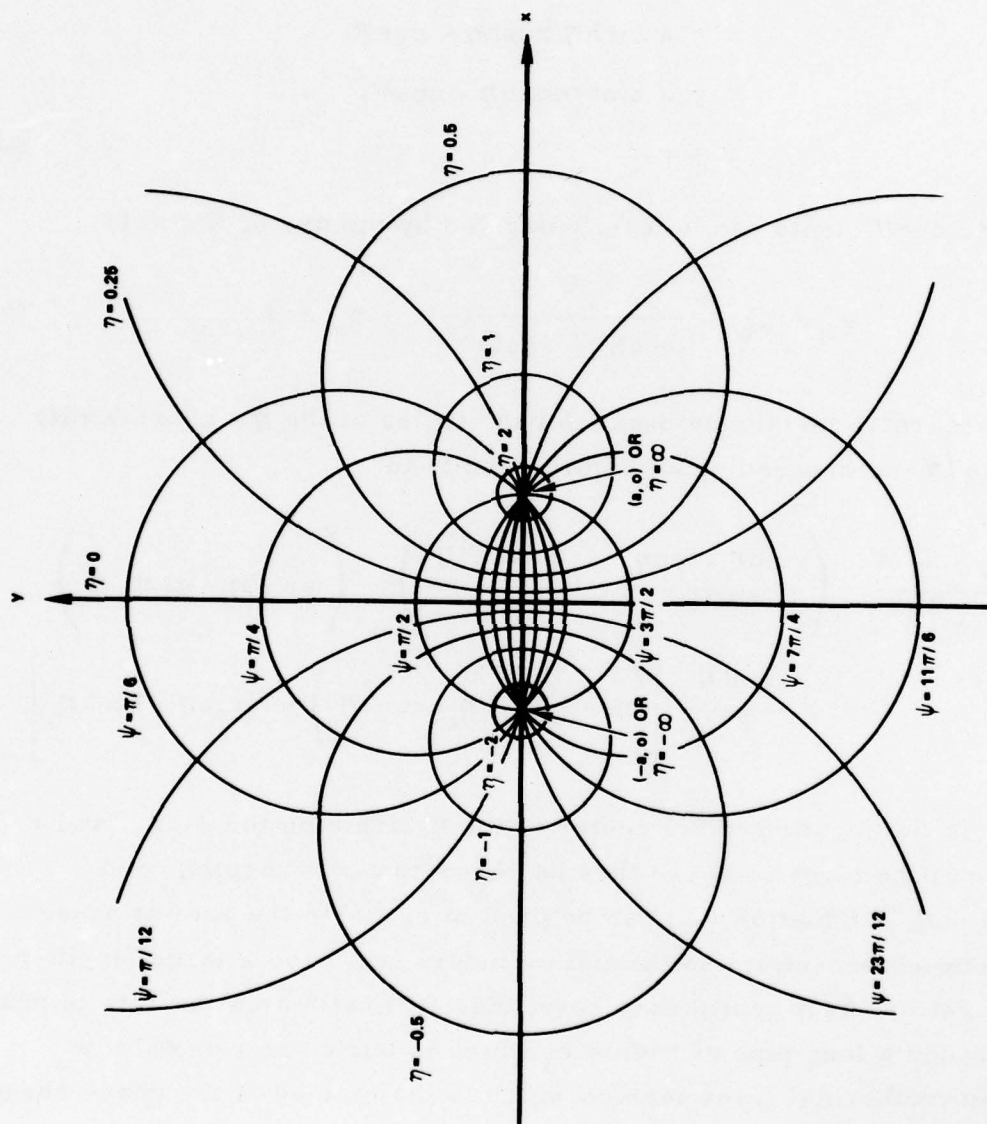


Fig. 10. Bicyclic Coordinates

the y -axis. The relation between bipolar coordinates and Cartesian coordinates is¹³

$$\begin{aligned}x &= a \sinh \eta / (\cosh \eta - \cos \psi) \\y &= a \sin \psi / (\cosh \eta - \cos \psi) \\z &= z\end{aligned}\tag{60}$$

The metric coefficients can be easily derived by the use of Eq. (11)

$$g_{\eta} = g_{\psi} = \frac{a^2}{(\cosh \eta - \cos \psi)^2}, \quad g_z = 1\tag{61}$$

Using the thermal resistance between two circles of the $\eta = \text{const}$ family $(\eta_o - \eta)/2k\ell\pi$ and proceeding as before results in

$$\begin{aligned}\frac{k(T_{fr} - T_o)t}{\rho L w_o^2} &= \left(\frac{\sinh \eta_o \tanh \eta_o}{2Bi} + \frac{\eta_o \tanh^2 \eta_o}{2} \right) \cdot \left(\text{csch}^2 \eta - \text{csch}^2 \eta_o \right) \\&\quad - \frac{\tanh^2 \eta_o}{2} \left[\left(\eta \text{csch}^2 \eta - \eta_o \text{csch}^2 \eta_o \right) + \text{ctnh} \eta - \text{ctnh} \eta_o \right]\end{aligned}\tag{62}$$

where w_o is the location of the center of the η -circle on the x -axis and r_o is the radius of the circle. It can thus be shown that $w_o = a \coth \eta_o$ and $r_o = a / |\sinh \eta_o|$. Equation (62) can be used to estimate the rate of phase change between eccentric isothermal cylinders that have a large length-to-diameter ratio. As η approaches zero, Eq. (62) estimates the rate of phase change around a long pipe of radius r_o which is buried at a depth of w_o beneath an isothermal level surface which is maintained at the phase change temperature.

G. ESTIMATION OF ERRORS

An estimate of the error caused by neglecting the heat capacity of the solidified (or melted) portion cannot be readily determined for the case of the elliptic cylinder and spheroidal coordinates. However, since the solutions obtained are bracketed by, and similar to, the more common cases of the one-dimensional slab and the cylinder, it is reasonable to assume that an analysis of the error involved in these cases will indicate the error involved in the more complex geometrics treated herein. Goodman,² using the heat-balance integral, obtained a solution for the slab problem shown in Figs. 1b and 1d with $h_o \sim \infty$ and $x_o = 0$. His result for the location of the phase change front is

$$x = (\sqrt{1 + 2 \text{Ste}} - 1)^{1/2} \sqrt{2\alpha t} \quad (63)$$

which approximates the exact solution given in Carslaw and Jaeger¹ within 2.0% up to $\text{Ste} = 0.5$. The comparable solution for the case of negligible heat capacity can be obtained by letting h_o approach infinity, taking $x_o = 0$ in Eq. (8), and carrying out the simple integration. The result is

$$x = \sqrt{\text{Ste}} \sqrt{2\alpha t} \quad (64)$$

The percent error in calculating the time required to reach a given location of the phase-change front can be obtained by comparing Eqs. (63) and (64) (see Fig. 11). Ignoring the heat capacity results in change of phase times that are always shorter, as expected. As long as the Stefan number is below 0.2, Eq. (64) underpredicts the phase-change time by less than 10%. For Stefan numbers below 0.05 the maximum error is below 3%.

Further confirmation of the validity of neglecting the sensible heat effects for low Stefan numbers was carried out by comparing Megerlin's⁵ result for a cylinder, given below, with Eqs. (38) and (39).

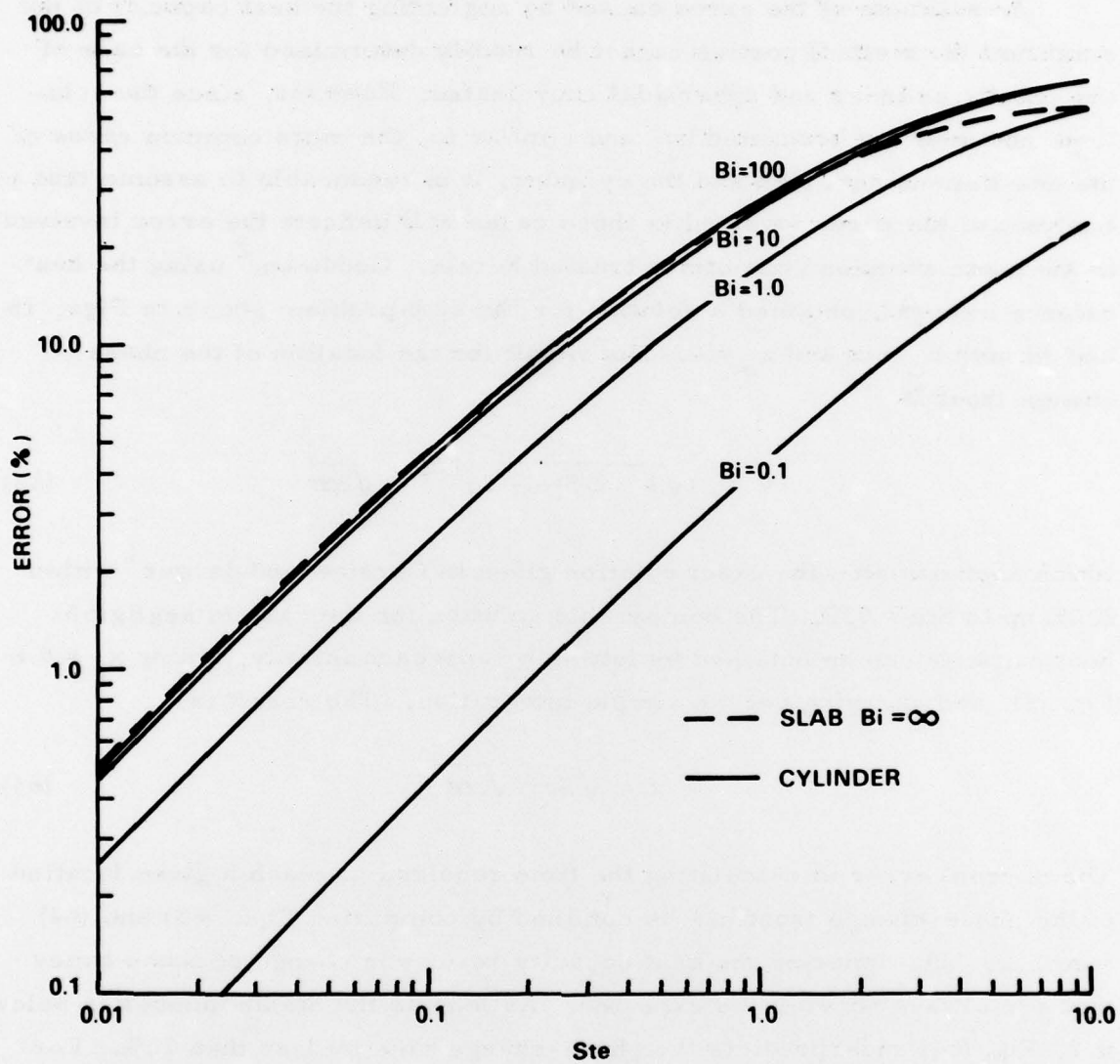


Fig. 11. Percent Error in $SteFo$ due to Neglecting the Sensible Heat Effect as a Function of Stefan Number with Biot Number as a Parameter

$$\text{SteFo}_{C \neq 0} = \int_{r^*}^1 \frac{r^*}{2\text{Bi}} \left[\sqrt{(1 - \text{Bi} \ln r^* - 2 \text{SteBi} \ln r^* (2 - \text{Bi} \ln r^*) + (1 - \text{Bi} \ln r^*)^2)} \right] dr^* \quad (65)$$

$$\frac{T_w - T_o}{T_{fr} - T_o} = \frac{1}{\text{Ste}} \left[r^* \ln r^* + \frac{1}{2} (r^*)^2 (\ln r^*)^2 \right] \quad (66)$$

where

$$r^* = \frac{-2\text{SteBi}}{r^* \left[\sqrt{(1 - \text{Bi} \ln r^*)^2 - 2\text{SteBi} \ln r^* (2 - \text{Bi} \ln r^*) + (1 - \text{Bi} \ln r^*)^2} \right]}$$

These equations, although approximate, have been shown to yield results of high accuracy by comparison with finite difference solutions.¹⁶ The percent error as a function of Stefan number has been calculated and is shown in Fig. 11 with Biot number as a parameter. The percent error is defined by $100(\text{SteFo}_{C \neq 0} - \text{SteFo}_{C=0})/\text{SteFo}_{C \neq 0}$. Lower Biot numbers tend to decrease the error in neglecting the sensible heat effects. The integration of Eq. (65) was carried out numerically using Simpson's method with interval-halving and a convergence criterion of 0.5×10^{-5} between iterations. The error in comparing the wall temperature as predicted by Eqs. (66) and (39) is about the same as above for Stefan numbers up to 1.0. For larger Stefan numbers the error is less than the error in SteFo .

H. FLUX BOUNDARY CONDITION

When the heat transfer rate is specified at the container wall the heat balance Eq. (23) simplifies considerably to

$$Q = \rho L \frac{d}{dt} (V_o - V) \quad (67)$$

¹⁶Shamsundar, N., and Sparrow, E.M., "Storage of Thermal Energy by Solid-Liquid Phase-Change--Temperature Drop and Heat Flux," Journal of Heat Transfer, Trans. ASME, Series C, Vol. 96, pp. 541-543.

for the inward phase change problem subject to the same assumptions stated earlier. The wall temperature can also be readily calculated from $Q = (T_{fr} - T_w)/R$ by substituting $\bar{q}_o A_o$ for Q and using the appropriate thermal resistance for the coordinate system used. The results are summarized in Table 1. The symbol c represents the half thickness x_o for the case of a slab, the outer radius r_o for the cylinder and sphere, and the semiminor axis for the remaining coordinate systems. The symbol F is related to η by the same equations as for the convection boundary condition cases described earlier. Figure 12 shows the calculated results for selected geometric shapes. The frozen fraction is a linear function of the dimensionless time parameter used for all cases; the dimensionless temperature difference, however, is nonlinear and tends to high values for some geometries at the end of the phase change period. For applications where low temperature differences are required, elliptic cylinders, oblate spheroids, and slabs are more appropriate phase change container shapes than spheres, cylinders and prolate spheroids. The reason is that the thermal resistance between the container wall and its center tends to infinity for certain geometries, thus resulting in high temperature differences.

Note that the equations presented in Table 1 are derived from thermal resistances based on isothermal boundary conditions. For uniform flux boundary conditions the problem becomes generally two-dimensional; however, departures from one-dimensionality are expected to be small because of the symmetry of the problems considered herein. The symbol \bar{q} should be interpreted as the area-averaged heat transfer rate so that the boundary condition temperature is uniform. This is believed to be a valid approach since in most real situations the actual boundary condition is not known exactly and usually lies somewhere between the constant temperature and the constant flux condition. For the case of bipolar coordinates where highly asymmetric geometries are involved, large departures from one-dimensionality are present for certain uniform flux cases as reported in Ref. 17.

¹⁷Thiyagarajan, R., and Yovanovich, M.M., "Thermal Resistance of a Buried Cylinder with Constant Flux Boundary Condition," Journal of Heat Transfer, Trans. ASME, Series C, Vol. 96, pp. 249-250.

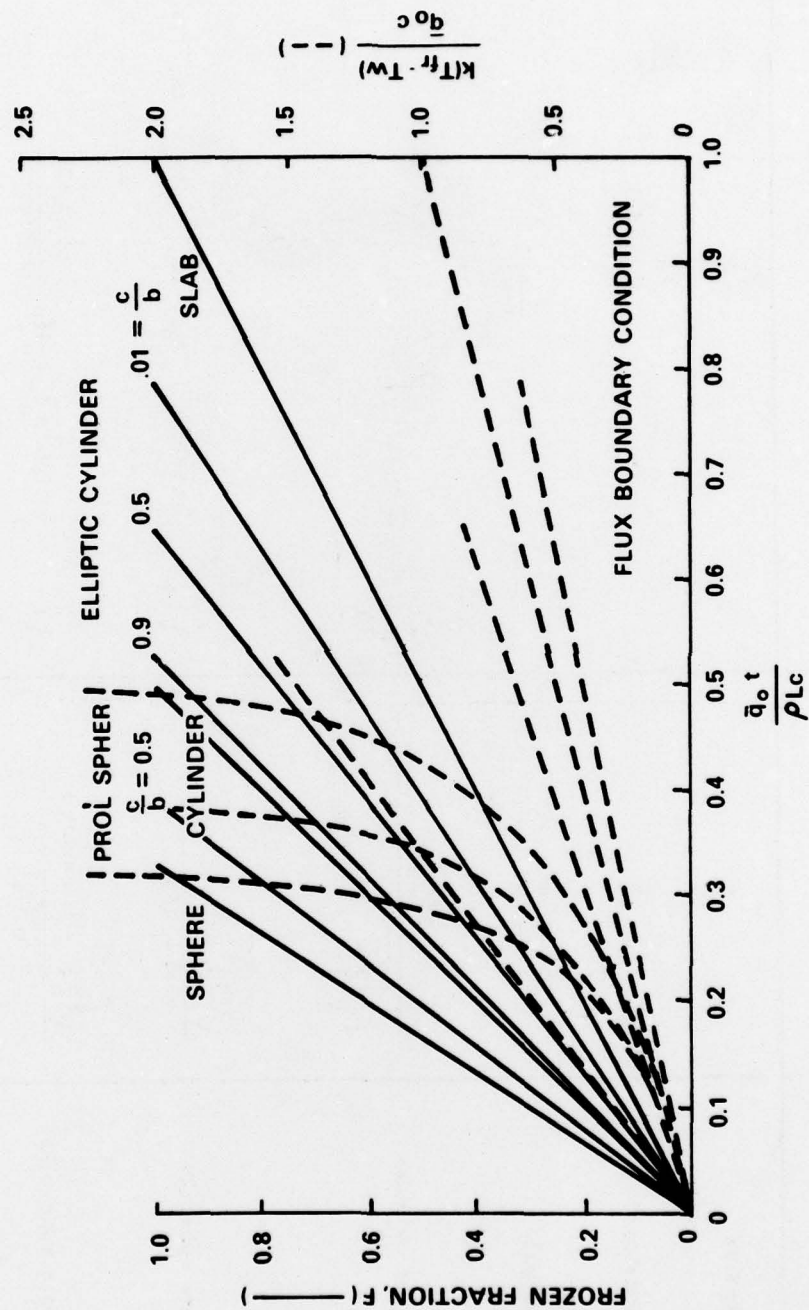


Fig. 12. Frozen Fraction and Dimensionless Temperature Difference as a Function of Time for Several Geometries

Table 1. Flux Boundary Condition Equations

Coordinate System	$\frac{\bar{q}_o t}{\rho L c}$	$\frac{k(T_{fr} - T_w)}{\bar{q}_o c}$
Cartesian	F	F
Cylindrical	$\frac{F}{2}$	$-\ln r^*$
Spherical	$\frac{F}{3}$	$\frac{1}{r^*} - 1$
Elliptic cylinder	$\frac{\pi \left(\frac{b}{c}\right) F}{4 \sqrt{\left(\frac{b}{c}\right)^2 - 1} \cosh \eta_o E(\eta_o)}$	$\frac{2}{\pi} \cosh \eta_o E(\eta_o) \sqrt{\left(\frac{b}{c}\right)^2 - 1} (\eta_o - \eta)$
Oblate spheroidal	$\frac{\sqrt{\left(\frac{b}{c}\right)^2 - 1} \sinh \eta_o F}{3 I_o(\eta_o)}$	$\sqrt{\left(\frac{b}{c}\right)^2 - 1} \cosh^2 \eta_o I_o(\eta_o) [\tan^{-1}(\sinh \eta_o) - \tan^{-1}(\sinh \eta)]$
Prolate spheroidal	$\frac{\sqrt{\left(\frac{b}{c}\right)^2 - 1} \cosh \eta_o F}{3 I_p(\eta_o)}$	$\sqrt{\left(\frac{b}{c}\right)^2 - 1} \sinh^2 \eta_o I_p(\eta_o) \ln \frac{\tanh(\eta_o/2)}{\tanh(\eta/2)}$

I. APPROXIMATION OF TWO-DIMENSIONAL PROBLEMS

Sometimes it is possible to approximate the thermal behavior of two- and three-dimensional phase change problems by a one-dimensional analysis using an appropriate coordinate system. Table 2 lists a comparison of the wall temperature ratio and dimensionless time parameter for different frozen fractions as calculated by Eqs. (38) and (39) with the numerical results obtained in Ref. 12 where an ad hoc computer program was used to predict the rates of freezing and temperature distributions of a PCM contained in a convectively cooled square container. The maximum error is 10% for this case where $Biot = 1.0$. The maximum error calculated for the $Biot = 10.0$ and $Biot = 0.1$ cases are 17 and 2.6%, respectively. Another example is the two-dimensional problem of a long cylinder of finite length that can be approximated by using prolate spheroidal coordinates where c/b approaches zero.

Table 2. Comparison of Eqs. (38) and (39) with the Numerical Results of Ref. 12 for Biot = 1.0

Frozen Fraction	$(T_w - T_o)/(T_{fr} - T_o)$		SteFo	
	Eq. (39)	Ref. 12	Eq. (38)	Ref. 12
0.097	0.9515	0.95	0.04972	0.05
0.189	0.9052	0.905	0.0993	0.10
0.274	0.8620	0.865	0.1474	0.15
0.428	0.7817	0.815	0.2410	0.25
0.564	0.7067	0.75	0.3325	0.35
0.738	0.5989	0.64	0.4658	0.50
0.878	0.4874	0.51	0.5940	0.65
0.983	0.3292	0.36	0.7199	0.80

III. DISCUSSION AND CONCLUSIONS

A general expression for predicting the rates of melting or freezing and the resulting temperature histories was presented, based on the conduction shape factor equation derived in Refs. 13 or 15 and the assumptions adopted by London and Seban⁷, concerning the phase change process. Closed-form solutions were obtained for elliptic cylinder, oblate spheroidal, prolate spheroidal coordinates, and bicylindrical coordinates. Arithmetic results were presented in graphical form for the inward phase change problem in some of these coordinate systems. These results are of special interest to the design of thermal storage equipment where container wall temperatures and heat flow rates for various container shapes are important as is the location of the solid-liquid interface. Elliptic cylinders and oblate spheroids of medium to high eccentricities that resemble a slab-like geometry were shown to give lower temperature differences and more uniform heat flow rates than cylinders, spheres, and prolate spheroids. Low Biot numbers resulted in more uniform heat extraction rates and low temperature differences; however, longer times are required for complete phase change. The error involved in neglecting the sensible heat effects was computed in order to assess the limits of applicability of the results presented. The maximum expected error was determined to be less than 10% for Stefan numbers below 0.2 and 3% for Stefan numbers less than or equal to 0.05.

The large number of other applications where the solution technique can be used is of far greater significance than the few examples calculated herein. For example, freezing around a disc-shaped cryoprobe can be estimated by using the expressions presented in oblate spheroidal coordinates in an outward direction. Freezing or melting around a finite plate immersed in a semi-infinite medium can be estimated by the elliptic cylinder results in an outward direction. Other cases such as melting or freezing around buried cylinders or spheres can be treated by the use of bicylinder and bispherical coordinate systems, respectively.

REFERENCES

1. Carslaw, H.S., and Jaeger, J.C., Conduction of Heat in Solids, 2nd ed., Oxford University Press, London and New York, 1959.
2. Goodman, T.R., "The Heat-Balance Integral and Its Application to Problems Involving a Change of Phase," Transactions of ASME, Vol. 80, 1958, pp. 335-342.
3. Biot, M.A., and Daughaday, H., "Variational Analysis of Ablation," Journal of Aerospace Sciences, Vol. 29, No. 2, 1962, pp. 227-228.
4. Rosenthal, D., "The Theory of Moving Sources of Heat and Its Application to Metal Treatments," Transactions of ASME, Vol. 68, 1946, pp. 849-866.
5. Megerlin, F., "Geometrisch eindimensionale Wärmeleitung beim Schmelzen und Erstarren," Forsch. Ing. -Wes., Vol. 34, 1968, pp. 40-46.
6. Lin, S., "An Analytical Method for Solving Geometric One-dimensional Freezing or Melting Problems," ASME Paper No. 73-WA/HT-33.
7. London, A. L., and Seban, R.A., "Rate of Ice Formation," Transactions of the ASME, Vol. 6, 1943, pp. 771-778.
8. Ehrlich, L.W., "A Numerical Method of Solving a Heat Flow Problem with Moving Boundary," Journal of ACM, Vol. 5, 1958, pp. 161-176.
9. Murray, W.D., and Landis, F., "Numerical and Machine Solutions of Transient Heat-Conduction Problems Involving Melting or Freezing," Transaction of ASME, Vol. 81, 1959, pp. 106-112.
10. Poots, G., "An Approximate Treatment of Heat Conduction Problem Involving a Two-Dimensional Solidification Front," International Journal of Heat and Mass Transfer, Vol. 5, 1962, pp. 339-348.
11. Rathjen, K.A., and Jiji, L.M., "Heat Conduction with Melting or Freezing in a Corner," Journal of Heat Transfer, Trans. ASME, Series C, Vol. 93, 1971, pp. 101-109.
12. Shamsundar, N., and Sparrow, E.M., "Analysis of Multidimensional Conduction Phase Change Via the Enthalpy Model," Journal of Heat Transfer, Trans. ASME, Series C, Vol. 97, 1975, pp. 333-340.

REFERENCES (Continued)

13. Yovanovich, M.M., Advanced Heat Conduction, Hemisphere Publishing Corporation, Washington, D.C., 1978.
14. Moon, P., and Spencer, D.E., Field Theory for Engineers, D. Van Nostrand Company, Inc., Princeton, New Jersey, 1961.
15. Yovanovich, M.M., "A General Expression for Predicting Conduction Shape Factors," AIAA Paper No. 73-121.
16. Shamsundar, N., and Sparrow, E.M., "Storage of Thermal Energy by Solid-Liquid Phase-Change--Temperature Drop and Heat Flux," Journal of Heat Transfer, Trans. ASME, Series C, Vol. 96, pp. 541-543.
17. Thiyagarajan, R., and Yovanovich, M.M., "Thermal Resistance of a Buried Cylinder with Constant Flux Boundary Condition," Journal of Heat Transfer, Trans. ASME, Series C, Vol. 96, pp. 249-250.

NOMENCLATURE

A	surface area of container
a	focal length of ellipse
Bi	Biot number, hc/k
b	semimajor axis
C	specific heat
c	semiminor axis and specific heat
F	frozen fraction
Fo	Fourier number, $(k/\rho C x_0^2)t$
g	metric coefficient
h	convective heat transfer coefficient
k	thermal conductivity
L	latent heat of fusion
Q	total heat transfer rate
q	heat transfer rate per unit area
R	thermal resistance
r	radius of circular cylinder or sphere
r^*	dimensionless radius for cylinder or sphere
\dot{r}^*	time rate of change of solid-liquid interface radius
Ste	Stefan number, $C(T_{fr} - T_o)/L$
SteFo	Product of Stefan and Fourier numbers, $k(T_{fr} - T_o)t/\rho L r_o^2$
T	temperature
t	time

NOMENCLATURE (Continued)

u_1, u_2, u_3	orthogonal curvilinear coordinates
x, y, z	Cartesian coordinates
α	thermal diffusivity, $k/\rho C$
η, θ, z	elliptic cylinder coordinates
η, θ, ψ	oblate or prolate spheroidal coordinates
ρ	density
l	length

Subscripts

c	complete freezing or melting
i, j, k	corresponding to the coordinate i, j, or k
fr	freezing (or melting) temperature
o	outer wall for inward problems inner wall for outward problems